Research Article

Journal of PeptideScience

Received: 12 October 2010 Revised: 24 November 2010 Accepted: 1 December 2010 Published online in Wiley Online Library: 24 February 2011

(wileyonlinelibrary.com) DOI 10.1002/psc.1347

Low-generation asymmetric dendrimers exhibit minimal toxicity and effectively complex DNA

Neha Shah,[a,b] Raymond J. Steptoe[b]* and Harendra S. Parekh[a]*

Conventional dendrimers are spherical symmetrically branched polymers ending with active surface functional groups. Polyamidoamine (PAMAM) dendrimers have been widely studied as gene delivery vectors and have proven effective at delivering DNA to cells *in vitro*. However, higher-generation (G4-G8) PAMAM dendrimers exhibit toxicity due to their high cationic charge density and this has limited their application *in vitro* and *in vivo*. Another limitation arises when attempts are made to functionalize spherical dendrimers as targeting moieties cannot be site-specifically attached. Therefore, we propose that lower-generation asymmetric dendrimers, which are likely devoid of toxicity and to which site-specific attachment of targeting ligands can be achieved, would be a viable alternative to currently available dendrimers. We synthesized and characterized a series of peptide-based asymmetric dendrimers and compared their toxicity profile and ability to condense DNA to spherical PAMAM G1 dendrimers. We show that asymmetric dendrimers are minimally toxic and condense DNA into stable toroids which have been reported necessary for efficient cell transfection. This paves the way for these systems to be conjugated with targeting ligands for gene delivery *in vitro* and *in vivo*. Copyright © 2011 European Peptide Society and John Wiley & Sons, Ltd.

Supporting information may be found in the online version of this article

Keywords: asymmetric dendrimers; toroids; low-generation peptides; cytotoxicity; PAMAM G1

Introduction

Dendrimers such as polyamidoamine (PAMAM) [1], polyethyleneimine (PEI) [2] and poly(L-lysine) (PLL) [3,4] have been used to facilitate delivery and expression of DNA [5], delivery of drugs and radiotherapeutics [6,7] and for *in vitro* and *in vivo* diagnostics [8]. Dendrimers are synthesized by either divergent [9] or convergent [10] approaches, each of which can give rise to linear or branched architectures, thus enabling the size and generation of the dendrimer to be controlled during synthesis. Commercially available dendrimers such as PAMAM and PEI are synthesized in solution by sequentially coupling 'layers' of repeating branched monomer units starting from a central core and ending with NH_2, OH, CHO, COOMe, Boc, COONa or CH_3 termini, the NH_2 typically being employed in gene delivery. The surface amine groups of PAMAM and other dendrimers interact with negatively charged molecules (e.g. DNA, oligonucleotide, siRNA) allowing dendrimers to protect and transport these molecules to a wide variety of cell types ([11]).

Of spherical dendrimers, PAMAM is the most widely used for *in vitro* gene delivery, with the primary focus being on the use of highly-branched ('high generation' G4–G8) dendrimers which are predicted to possess between 64 and 1024 surface amine termini [1,12,13]. High-generation PAMAM dendrimers have been found to facilitate more efficient transfection than the lower-generation dendrimers. For example, *in vitro* studies performed using PAMAM G6 dendrimers showed maximal transfection, whereas use of G10 dendrimers provided no significant increase in transfection efficiency [14] and PAMAM G2 dendrimers facilitate negligible plasmid DNA transfection relative to G4, G7 and G9 dendrimers [15]. PAMAM dendrimers modified with PEG or cyclodextrins have also been used to successfully achieve high-transfection efficiency *in vitro* [16].

Despite these results a major shortcoming of PAMAM dendrimers, that limits their use both *in vitro* and *in vivo* has been undesirable toxicity associated with their high-surface cationic charge density and the excess of positive charge associated with the high nitrogen (dendrimer) : Phosphate (DNA) ratios commonly employed [12,13]. For PAMAM dendrimers *in vitro,* cytotoxicity has been shown to be generation-dependent with the G5 and G7 higher-generation dendrimers exhibiting increasing cytotoxicity

* *Correspondence to: Dr Raymond J. Steptoe, The University of Queensland Diamantina Institute, Princess Alexandra Hospital, Level 4, R Wing, Building 1, Woolloongabba, QLD 4102, Australia. E-mail: r.steptoe@uq.edu.au*

** *Dr Harendra S. Parekh, School of Pharmacy, The University of Queensland, Brisbane, QLD 4102, Australia. E-mail: h.parekh@uq.edu.au*

a *School of Pharmacy, The University of Queensland, Brisbane, QLD 4102, Australia*

b *The University of Queensland Diamantina Institute, Princess Alexandra Hospital, Woolloongabba, QLD 4102, Australia*

Abbreviations used: *DNA, deoxyribonucleic acid; siRNA, short interfering ribonucleic acid; PEG, poly (ethylene glycol); H_2O, water; D_2O, deuterium oxide; CH_3CN, acetonitrile; HFBA, heptafluorobutyric acid; Fmoc, fluorenylmethoxycarbonyl; Pbf, 2,2,4,6,7-pentamethyldihydrobenzofuran-5-sulfonyl; DCM, dichloromethane; TIPS, triisopropyl silane; R_t, retention time; FCS, foetal calf serum; PBS, phosphate buffer saline; aq, aqueous; TFA, trifluoroacetic acid; SPPS, solid phase peptide synthesis; DIPEA, N, N-diisopropylethylamine; DMF, N, N-Dimethylformamide; RP-HPLC, reverse-phase high performance liquid chromatography.*

over G3 dendrimers [12] and higher-generation (≥G4) PAMAM dendrimers are approximately threefold more cytotoxic than G2 or G3 dendrimers [1]. Surface PEGylation of spherical dendrimers has been attempted to circumvent toxicity; however, this has led to a reduced number of active surface sites for gene complexation thereby limiting the effectiveness of these vectors [17,18]. For targeted delivery of DNA, another limitation of spherical PAMAM dendrimers is that there is a surplus of available reactive sites due to the stochastic synthesis. Therefore, it is not possible to attach targeting ligands in a site-specific manner or distal to the DNA complexing sites. Furthermore, PAMAM dendrimers are relatively expensive to manufacture, primarily due to the significant excess of monomer units required for traditional growth schemes, and the reduced purity of the desired end product obtained relative to solid-phase synthesis [19].

One approach to overcoming the limitations of spherical dendrimers would be development of low-generation, asymmetric dendrimers that could be prepared on an insoluble solid-support, for example, by a technique commonly referred to as solid phase peptide synthesis (SPPS) [20–22]. One advantage of SPPS is that low-generation asymmetric dendrimers can be synthesized rapidly, in high purity and yield [21,23]. We propose the low cationic charge of such dendrimers, even at high N:P ratios, would not predispose them to the cytotoxicity observed with higher generation of spherical dendrimers. By utilizing the well-established technique of SPPS, asymmetric dendrimers could be readily constructed to incorporate a well-defined site for a targeting ligand, using an orthogonal protecting strategy where a targeting ligand is site-specifically conjugated on a side-chain of the dendrimer distal to the DNA binding site [24]. Targeting moieties could be as diverse as antibodies [25], peptides and carbohydrates [26,27], depending on the target-cell of interest.

Here we describe an approach, using SPPS, for rapid synthesis of peptide-based low-generation asymmetric dendrimers. The physico-chemical characteristics of dendrimer-DNA binding, toxicity profile and morphology were compared for dendrimer/DNA complexes formed using either peptide-based asymmetric dendrimers or a commercially available PAMAM G1 dendrimer, for comparison.

Materials and Methods

Materials

All fluorenylmethyoxycarbonyl (Fmoc) amino acids and Rink amide resin (200–400 mesh) were purchased from NovaBiochem (Australia) unless otherwise stated. The solvent employed throughout the synthesis was peptide grade *N*, *N*-Dimethylformamide (DMF) (Merck) used without further purification. PAMAM G1, piperidine, trifluoroacetic acid (TFA) and ethidium bromide were purchased from Sigma–Aldrich. Dulbecco's modified Eagle's medium (DMEM) and Lipofectamine® were purchased from Invitrogen.

Instrumentation

Purification of asymmetric dendrimers was performed by reverse-phase high performance liquid chromatography (RP-HPLC). Preparative RP-HPLC was performed on a Waters HPLC system (Model 600 controller, 2996 photodiode array detector) with a C_4 column (Vydac, 5 μm pore size, id = 4.6 mm, 250 mm). Dendrimers were injected (~100 mg/batch) using a flow rate of 10 ml/min, isocratic conditions (100% A) and purified with the mobile phase comprising solvent A (100% H_2O), solvent B (90% $CH_3CN_{(aq)}$).

Analytical RP-HPLC was performed using a Shimadzu HPLC system (controller – CBM-20A, pump A – LC-10AD, autosampler – SIL-10AXL, detector – SPD-10A) with a C_4 column and mobile phase comprised solvent A (0.02% $HFBA_{(aq)}$) [28] and solvent B [90% $CH_3CN_{(aq)}$]. Analysis of each purified asymmetric dendrimer was undertaken at a flow rate of 1 ml/min, using the following conditions: 100% A (0–20 min), then to 100% B linearly over 10 min.

Liquid chromatography/mass spectrometry (LC–MS) was performed using an Applied Biosystems/MDS Sciex Q-TRAP LC/MS/MS system. For ESI^+-MS, each asymmetric dendrimer was dissolved in 50% $CH_3CN_{(aq)}$ to 300 μg/ml and observed for the molecular ion.

NMR spectroscopy was performed using a Bruker Topsin 400/500 NMR spectrometer (400/500 MHz). Each asymmetric dendrimer was dissolved in D_2O with one or two drops of dioxane as an internal reference for ^{13}C NMR and dendrimer assignments confirmed with the aid of one and two-dimensional NMR.

Asymmetric Dendrimer Synthesis

Asymmetric dendrimers were synthesized as previously described [29], on a 0.5 mmol scale using Fmoc SPPS [21,30]. Rink amide resin (0.6 mmol/g loading capacity) was swollen in DMF in a sintered glass vessel for 60 min followed by Fmoc deprotection with 20% *v*/*v* piperidine in DMF (2 × 8 min washes). All amino acids were pre-activated before coupling using *O*-benzotriazole-*N*, *N*, *N*′, *N*′-tetramethyl-uronium-hexafluoro-phosphate (HBTU; 0.5 M in DMF) and *N*, *N*-diisopropylethylamine (DIPEA). Each coupling step was monitored for ninhydrin values of ≥99% using a quantitative color test devised to detect the presence of free amino groups spectrophotometrically [31], the Fmoc group was then deprotected as outlined above. The Rink amide resin was treated with Fmoc-protected amino acids [except for arginine which is both Fmoc and Pbf (2,2,4,6,7-pentamethyldihydrobenzofuran-5-sulfonyl) protected] in the following sequence:

4^+ *Arginine* (Figure 1–2): Glycine (Gly) (3 equiv.), Gly (2 equiv), Gly (2 equiv), Lysine (Lys) (2 equiv) and Arginine (Arg) (5 equiv). Terminal Fmoc-protected groups were deprotected using 20% *v*/*v* piperidine in DMF, the resin was then washed with DCM and dried *in vacuo*. The Pbf protecting group was removed during acidolytic cleavage of the dendrimers off-resin using TFA : DCM : H_2O : TIPS (90 : 5 : 2.5 : 2.5; 3 h). The mixture was filtered and TFA removed *in vacuo*. The mixture was then co-evaporated with toluene (3 × 15 ml), and triturated with ice cold diethyl ether. The dendrimer (crude) was reconstituted in water and lyophilized. ^1H NMR (D_2O) δ (ppm): 1.30–1.85 (Rβ, $R_1\beta$, Kβ, Kδ, Rγ, $R_1\gamma$, Kγ, C$\underline{H}_2$, 14H, m), 3.09–3.17 (Rδ, $R_1\delta$, Kδ, C$\underline{H}_2$, 6H, m), 3.76–3.93 (Rα, C$\underline{H}$, $G_{1-2}\alpha$, Gα, C$\underline{H}_2$, 7H, m), 3.96–3.99 ($R_1\alpha$, C$\underline{H}$, 1H, *t*, J = 6.61 Hz), 4.21–4.24 (Kα, C$\underline{H}$, 1H, *t*, J = 7.43 Hz). ^{13}C NMR (D_2O) δ (ppm): 23.59 (Kγ, C$\underline{H}_2$), 24.56 ($R_1\gamma$, C$\underline{H}_2$), 24.81 (Rγ, C$\underline{H}_2$), 29.8 (Kδ, C$\underline{H}_2$), 29.18 ($R_1\beta$, C$\underline{H}_2$), 29.27 (Rβ, C$\underline{H}_2$), 31.56 (Kβ, C$\underline{H}_2$), 40.46 ($R_1\delta$, C$\underline{H}_2$), 41.50 (Rδ, C$\underline{H}_2$), 41.61 (Kε, C$\underline{H}_2$), 43.19 (Gα, C$\underline{H}_2$), 43.58 ($G_1\alpha$, C$\underline{H}_2$), 43.65 ($G_2\alpha$, C$\underline{H}_2$), 53.71 ($R_1\alpha$, C$\underline{H}$), 54.14 (Rα, C$\underline{H}$), 55.45 (Kα, C$\underline{H}$), 158.01 (R2, $R_1$2, C$\underline{=}$NH), 170.45–170.91 (R, R_1, C$\underline{=}$O), 173.10 (G_{1-2}, G, C$\underline{=}$O), 175.49 (K, C$\underline{=}$O). Yield: 0.065 g (65%). ESI^+-MS *m*/*z*: ($C_{24}H_{48}N_{14}O_6$) calculated 628.39, found 629.50 $[M + H]^+$. R_t: 11.35 min.

8^+ *Arginine* (Figure 1–3): Gly (3 equiv), Gly (2 equiv), Gly (2 equiv), Lys (2 equiv), Lys (3 equiv) and Arg (6 equiv). The same process was followed as outlined for 4^+ Arginine above. ^1H NMR (D_2O) δ (ppm): 1.23–1.83 (Kγ, $K_{1-2}\gamma$, Kδ, $K_{1-2}\delta$, Rγ, $R_{1-3}\gamma$, Kβ, $K_{1-2}\beta$, Rβ, $R_{1-3}\beta$, C$\underline{H}_2$, 34H, m), 3.06–3.13 (Kε, $K_{1-2}\varepsilon$, Rδ, $R_{1-3}\delta$,

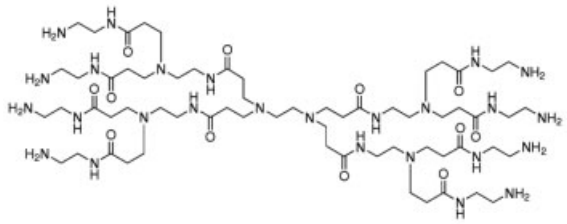

PAMAM G1, **1**

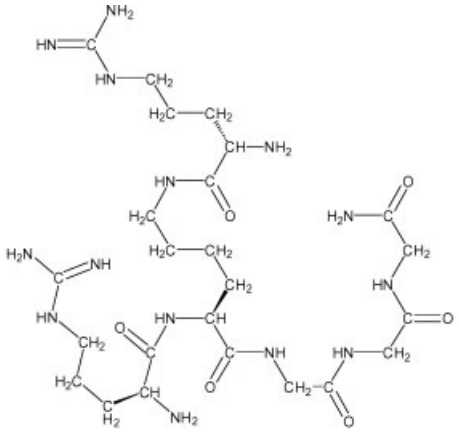

4^+ Arginine, **2**

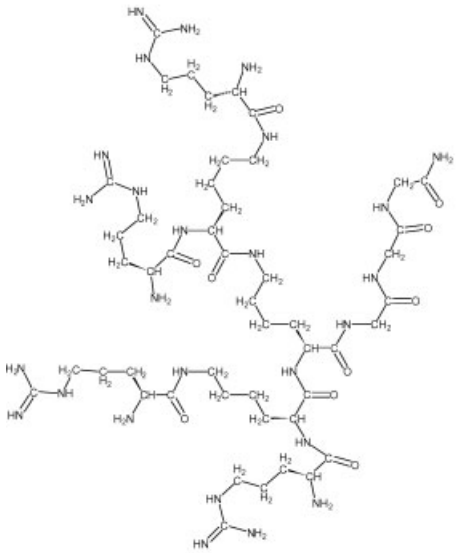

8^+ Arginine, **3**

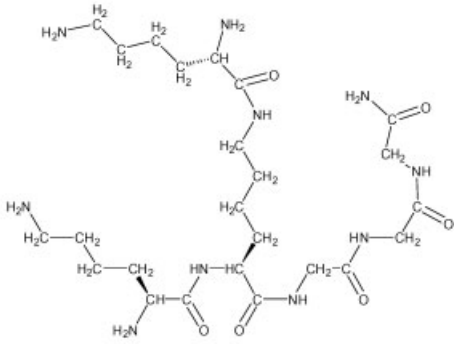

4^+ Lysine, **4**

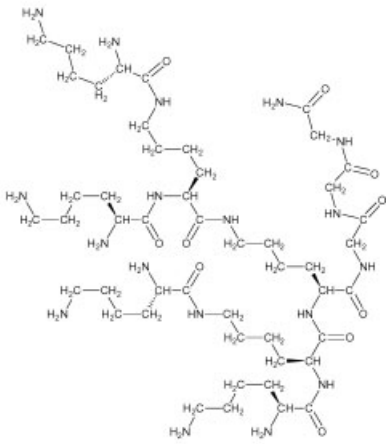

8^+ Lysine, **5**

Figure 1. Structure of PAMAM G11, 4^+ Arginine 2, 8^+ Arginine 3, 4^+ Lysine 4 and 8^+ Lysine 5 dendrimers.

$C\underline{H}_2$, 14H, m), 3.82 (Gα, $C\underline{H}_2$, 2H, s), 3.90 ($G_{1-2}\alpha$, $C\underline{H}_2$, $R_{1-3}\alpha$, $C\underline{H}$, 6H, s), 3.95–4.00 (Rα, $C\underline{H}$, 2H, m), 4.11–4.22 ($K_{1-2}\alpha$, Kα, $C\underline{H}$, 3H, t, $J = 7.30$ Hz). ^{13}C NMR (D_2O) δ (ppm): 23.62–23.75 (Kγ, $K_{1-2}\gamma$, $\underline{C}H_2$), 24.65–24.81 (Rγ, $R_{1-3}\gamma$, $\underline{C}H_2$), 28.98–29.26 (Rβ, $R_{1-3}\beta$, Kδ, $K_{1-2}\delta$, $\underline{C}H_2$), 31.67–31.74 (Kβ, $K_{1-2}\beta$, $\underline{C}H_2$), 40.29–40.50 (Rδ, $R_{1-3}\delta$, $\underline{C}H_2$), 41.49–41.62 (Kε, $K_{1-2}\varepsilon$, $\underline{C}H_2$), 43.23–43.72 (Gα, $G_{1-2}\alpha$, $\underline{C}H_2$), 53.71 ($R_{1\&3}\alpha$, $\underline{C}H$), 54.14 (Rα, $R_2\alpha$, $\underline{C}H$), 55.10 ($K_2\alpha$, $\underline{C}H$), 55.28 ($K_1\alpha$, $\underline{C}H$), 55.67 (Kα, $\underline{C}H$), 158.01 (R, $R_{1-3}2$, $\underline{C}$=NH), 170.45–170.77 (R, R_{1-2}, $\underline{C}$=O), 173.17–173.19 (G, G_{1-2}, $\underline{C}$=O), 174.57 (K_2, $\underline{C}$=O), 174.91 (R_3, $\underline{C}$=O), 175.33 (K, $\underline{C}$=O), 175.75 (K_1, $\underline{C}$=O). Yield: 0.063 g (63%).

Journal of PeptideScience

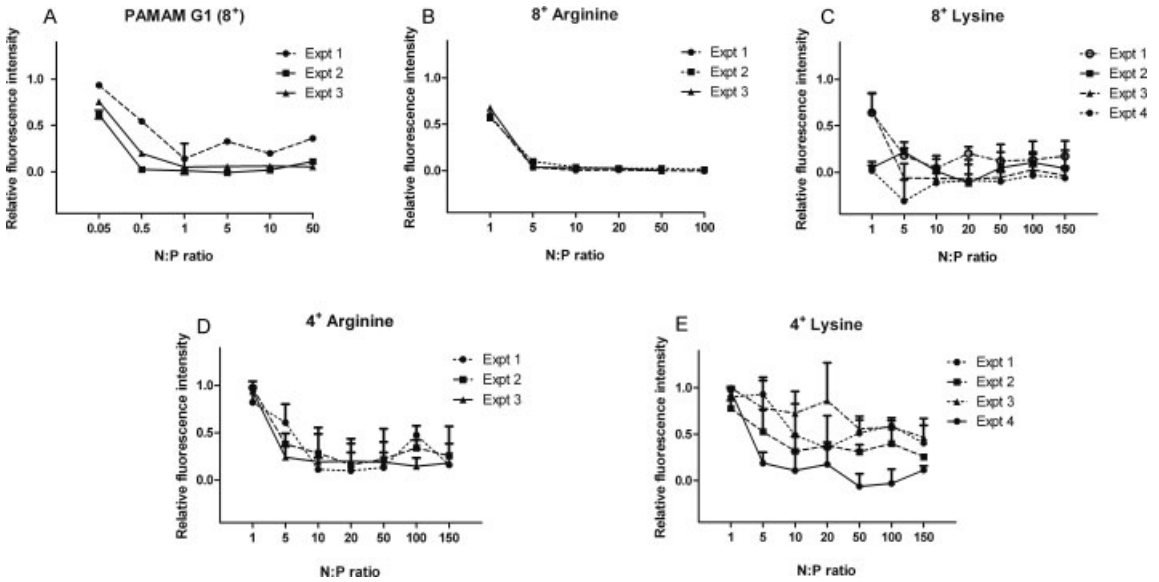

Figure 2. EtBr assay indicates effective DNA complexation by asymmetric dendrimers. Dendrimers were complexed with DNA in either Baxter or de-ionized water at increasing N : P ratio and equilibrated with EtBr : DNA base pair at a ratio of 1 : 4. Fluorescence was measured at 485 nm (Ex) and 590 nm (Em) or 544 nm (Ex) and 590 nm (Em) for triplicate samples in each assay and the relative fluorescence intensity calculated. Data from 2–4 separate experiments are shown as mean and SD of triplicate samples at each N : P ratio.

ESI$^+$-MS *m/z*: ($C_{48}H_{96}N_{26}O_{10}$) calculated 1197.44, found 1198.00 $[M + H]^+$. R_t: 13.28 min.

4$^+$ Lysine (Figure 1–4): Gly (3 equiv), Gly (2 equiv), Gly (2 equiv), Lys (2 equiv) and Lys (3 equiv). The same process was followed as outlined for 4$^+$ Arginine above. ^{1}H NMR (D_2O) δ (ppm): 1.21–1.85 (Kγ, $K_{1-2}\gamma$, Kδ, $K_{1-2}\delta$, Kβ, $K_{1-2}\beta$, C$\underline{H}_2$, 18H, m), 2.86–2.89 ($K_{1-2}\varepsilon$, C$\underline{H}_2$, 4H, m), 3.10–3.13 (Kε, C$\underline{H}_2$, 2H, t, J = 7.18 Hz), 3.77–3.93 ($K_{1-2}\alpha$, C$\underline{H}$, Gα, $G_{1-2}\alpha$, C$\underline{H}_2$, 8H, m), 4.21–4.24 (Kα, C$\underline{H}$, 1H, t, J = 7.18 Hz). ^{13}C NMR (D_2O) δ (ppm): 22.25 ($K_1\gamma$, C$\underline{H}_2$), 22.56 ($K_2\gamma$, C$\underline{H}_2$), 23.58 (Kγ, C$\underline{H}_2$), 27.60 ($K_1\delta$, $K_2\delta$, C$\underline{H}_2$), 29.11 (Kδ, C$\underline{H}_2$), 31.60 ($K_{1-2}\beta$, C$\underline{H}_2$), 31.65 (Kβ, C$\underline{H}_2$), 40.20 ($K_{1-2}\varepsilon$, C$\underline{H}_2$), 40.48 (Kε, C$\underline{H}_2$), 43.18 (Gα, C$\underline{H}_2$), 43.56 ($G_1\alpha$, C$\underline{H}_2$), 43.65 ($G_2\alpha$, C$\underline{H}_2$), 53.93 ($K_2\alpha$, C$\underline{H}_2$), 54.35 ($K_1\alpha$, C$\underline{H}$), 55.39 (Kα, C$\underline{H}$), 170.55–170.95 (K_{1-2}, C$\underline{=}$O), 173.06–173.14 (G, G_{1-2}, C$\underline{=}$O), 175.33–175.40 (K, C$\underline{=}$O). Yield: 0.083 g (83%). ESI$^+$-MS *m/z*: ($C_{24}H_{48}N_{10}O_6$) calculated 572.70, found 573.50 $[M + H]^+$. R_t: 10.29 min.

8$^+$ Lysine (Figure 1–5): Gly (3 equiv), Gly (2 equiv), Gly (2 equiv), Lys (2 equiv), Lys (3 equiv) and Lys (5 equiv). The same process was followed as outlined for 4$^+$ Arginine above. ^{1}H NMR (D_2O) δ (ppm): 1.25–1.79 (Kγ, $K_{1-6}\gamma$, Kδ, $K_{1-6}\delta$, Kβ, $K_{1-6}\beta$, C$\underline{H}_2$, 42H, m), 2.86–2.91 ($K_{1-6}\varepsilon$, C$\underline{H}_2$, 12H, q), 3.08–3.11 (Kε, C$\underline{H}_2$, 2H, m), 3.81–3.91 ($K_{3-6}\alpha$, C$\underline{H}$, Gα, $G_1\alpha$, $G_2\alpha$, C$\underline{H}_2$, 10H, m), 4.11 ($K_2\alpha$, C$\underline{H}$, 1H, t, J = 7.01 Hz), 4.15 ($K_1\alpha$, C$\underline{H}$, 1H, t, J = 7.01 Hz), 4.22 (Kα, C$\underline{H}$, 1H, t, J = 7.25 Hz). ^{13}C NMR (D_2O) δ (ppm): 22.38–22.57 ($K_{1-6}\gamma$, C$\underline{H}_2$), 23.67–23.76 (Kγ, C$\underline{H}_2$), 27.56–27.59 ($K_{1-6}\delta$, C$\underline{H}_2$), 29.16–29.22 (Kδ, C$\underline{H}_2$), 31.60–31.98 (Kβ, $K_{1-6}\beta$, C$\underline{H}_2$), 40.20–40.54 (Kε, $K_{1-6}\varepsilon$, C$\underline{H}_2$), 43.21–43.70 (Gα, $G_{1-2}\alpha$, C$\underline{H}_2$), 53.95 ($K_{4\&6}\alpha$, C$\underline{H}$), 54.36 ($K_{3\&5}\alpha$, C$\underline{H}$), 54.98 (Kα, C$\underline{H}$), 55.36 ($K_1\alpha$, C$\underline{H}$), 55.51($K_2\alpha$, C$\underline{H}$), 170.53–170.82 (K_1, C$\underline{=}$O), 173.11 (G, G_{1-2}, C$\underline{=}$O), 174.40 (K_2, C$\underline{=}$O), 174.81 (K, C$\underline{=}$O), 175.29 ($K_{3\&5}$, C$\underline{=}$O), 175.70 ($K_{4\&6}$, C$\underline{=}$O). Yield: 0.062 g (62%). ESI$^+$-MS *m/z*: ($C_{48}H_{96}N_{18}O_{10}$) calculated 1085.39, found 1086.00 $[M + H]^+$. R_t: 13.10 min.

Plasmid Preparation

Escherichia coli were transformed with a 4.7 kb plasmid (pEGFP-C1) encoding green fluorescent protein under control of a CMV promoter and grown in Luria broth (37 °C, 16 h) on a shaker at 300 rpm. Plasmid DNA was recovered using an endotoxin-free megaprep kit (Qiagen). DNA concentration was determined by UV absorbance at 260 and 280 nm after redissolving in water.

Ethidium Bromide Assay

DNA (pEGFP-C1, 0.2 µg) was mixed with dendrimer (1 mg/ml) at various N : P ratios in distilled water and incubated for 30 min at room temperature. After 30 min, ethidium bromide (EtBr) was added at an EtBr : DNA base pair ratio of 1 : 4 [32]. Fluorescence was measured (either 485 nm Ex, 590 nm Em or 544 nm Ex and 590 nm Em) using a FLUOstar Optima microplate reader (BMG Labtech Pty. Ltd., Victoria, Australia).

Transmission Electron Microscopy (TEM)

Dendrimer/DNA complexes were prepared as described above and, at defined times after mixing, stained as previously described [33]. Briefly, 400 mesh formvar-free carbon coated grids were glow discharged for 30 s. A 5 µl drop of dendrimer/DNA complex solution was carefully placed on the grid and immediately stained with 1% uranyl acetate and 15–30 s later excess liquid was wicked off with filter paper. Grids were air-dried before viewing (JEM – 1010 JEOL, Tokyo, 100 kV), images were captured using a digital camera (SoftImaging® Megaview III) and analyzed using SoftImaging®.

Cytotoxicity Assay

Human embryonic kidney 293T cells were grown in culture medium (DMEM 10% FCS) and seeded in a 24-well plate (3×10^6/well) in 500 µl of medium. Cells were incubated overnight (37 °C, 5% CO_2) to reach 50–60% confluency. Dendrimer/DNA complexes were prepared as described above and after 30 min incubation the solution was made isotonic by addition of 1/10 volume of 10 × PBS. The medium was then replaced by 500 µl

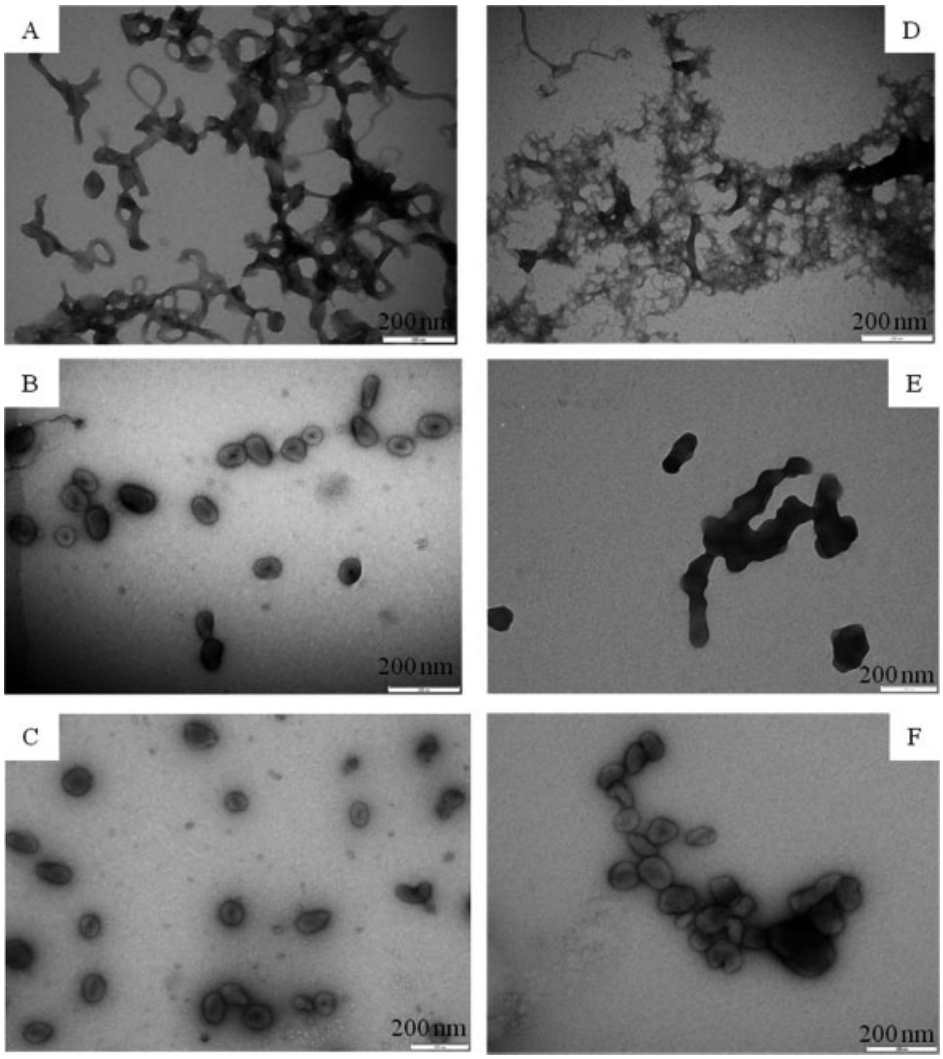

Figure 3. The difference in morphology of the structures indicates development of toroids at increasing N : P ratio. Dendrimer/DNA complexes were prepared in water (30 min incubation) and visualized by TEM. (A–C) PAMAM G1 1 : 1, 5 : 1 and 10 : 1 N : P ratios, respectively, (D–F) 8^+ Arginine at 1 : 1, 5 : 1 and 10 : 1 N : P ratios, respectively. Images are representative of at least ten sampled fields of view from each of three independent experiments carried out at each N : P ratio. Brightness and contrast on the images have been enhanced using Photoshop.

of fresh culture medium containing isotonic dendrimer solution. After an additional 4 h, dendrimer/DNA containing medium was replaced with fresh culture medium and cells cultured for a further 240 h. In the case of PAMAM G1, the dendrimer concentration added to cells ranged between 4 (for 5 : 1 N : P ratio) and 70 μg/ml (for 100 : 1 N : P ratio). Similarly, for 8^+ Arginine, the dendrimer concentration ranged between 3 (for 5 : 1 N : P ratio) and 59 μg/ml (for 100 : 1 N : P ratio). Lipofectamine® transfection was performed according to manufacturer's instructions and cultured for 24 h total. Non-adherent cells were harvested and pooled with adherent cells recovered by trypsinization. Viability was assessed by flow cytometry (BD FACScalibur™) after staining with propidium iodide.

Results

Synthesis and Characterization of Asymmetric Dendrimers

Asymmetric dendrimers with 4 or 8 terminal amines constructed with either arginine ('4^+ Arginine', '8^+ Arginine') or lysine ('4^+ Lysine', '8^+ Lysine') terminal amino acids (Figures 1–2 - 1–5) were synthesized using Fmoc SPPS. After purification using preparative RP-HPLC, all dendrimers were obtained in good yield (60–85%). The molecular weight of each dendrimer was confirmed by ESI^+-MS where the molecular ion of the dendrimer was identified. Both 1D and 2D NMR spectroscopy (^1H and ^{13}C) were used for definitive assignments of all synthesized dendrimers. The data confirmed successful synthesis of the panel of asymmetric dendrimers (Figures 1–2 - 1–5 and supporting information).

Assessment of DNA Complexation Using Ethidium Bromide Fluorescence

Ethidium bromide dye fluoresces when intercalated with DNA. As EtBr is prevented from intercalating with DNA in the presence of a complexing polycation, loss of fluorescence is a convenient measure of polycation/DNA complexation. On the basis of loss of fluorescence, PAMAM G1 effectively complexed DNA at N : P ratios $\geq$0.5 : 1 (Figure 2(A)). Of the four asymmetric dendrimers, 8^+ Arginine and 4^+ Arginine complexed DNA with the most reproducible results and at N : P ratios as low as 5 : 1 (Figure 2(B)

Journal of PeptideScience

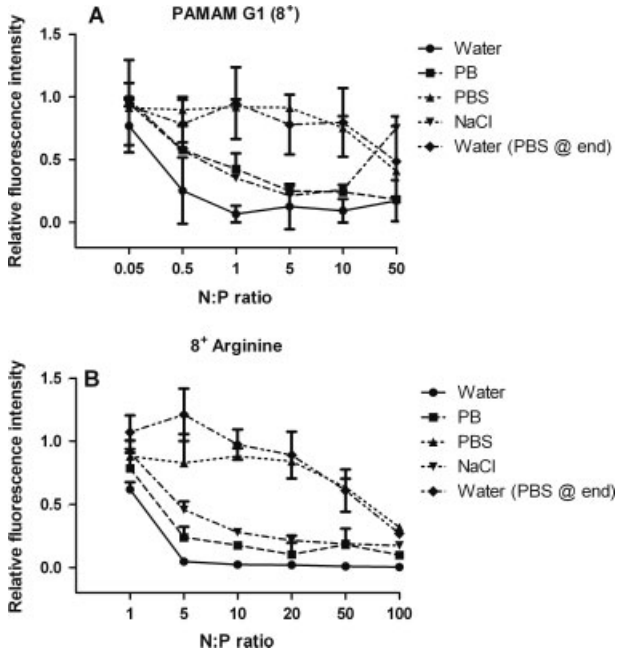

Figure 4. Dendrimer/DNA complexation is altered by the presence of sodium chloride ions. To determine the role of ions present in solution, PAMAM G1/DNA complexes (A) and 8^+ Arginine asymmetric dendrimer/DNA complexes (B) were prepared in different buffers and DNA complexation tested using the EtBr assay. Data (mean ± SD) are pooled from at least two independent experiments in which samples were tested in triplicate.

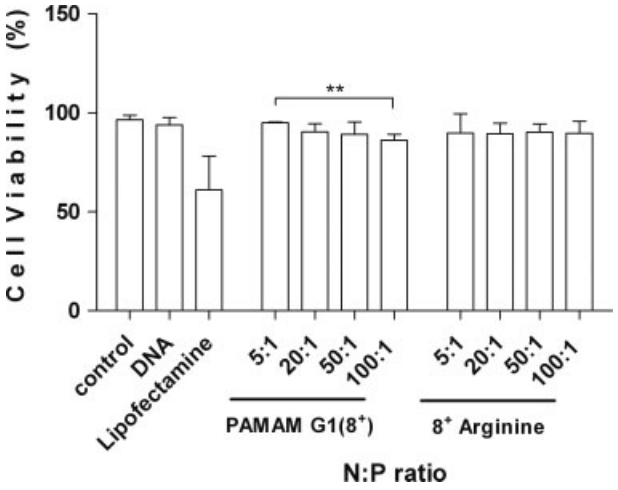

Figure 5. Low-generation dendrimers exhibit minimal cytotoxicity. Dendrimer/DNA complexes were prepared in water at defined N:P ratios, incubated for 30 min and then made isotonic by addition of 10 × PBS. Dendrimer/DNA complexes were then incubated with HEK 293T cells and cell viability assessed by propidium iodide staining 24 h later. Data (mean ± SD) are pooled from three independent experiments. Controls are untreated cells (control), cells incubated with DNA alone (DNA) or cells treated under identical conditions with DNA/Lipofectamine® complexes (Lipofectamine).

and (D)). 8^+ Lysine complexed DNA less reproducibly and at N:P ratios ≥5:1, whereas 4^+ Lysine least reproducibly complexed DNA (Figure 2(C) and (E)). Overall, asymmetric dendrimers constructed with arginine as the terminal amino acid complexed DNA more reproducibly, and at lower N:P ratios than those with lysine as the terminal amino acid.

Asymmetric Dendrimers form Toroidal Complexes with DNA

Transmission electron microscopy (TEM) was used to characterize the morphology of dendrimer/DNA complexes. Our aim was to investigate whether toroidal structures were formed as these have been reported as characteristic of DNA complexation in other polycationic systems [34,35]. For these studies, we chose to compare 8^+ Arginine, which possessed the most efficient DNA complexing characteristics in the EtBr assay, with PAMAM G1. At a 1:1 N:P ratio of PAMAM G1 to DNA, we observed a meshwork of pleiomorphic structures (Figure 3(A)). As the N:P ratio was increased to 5:1, individual rod and toroid-like structures, which often formed small clusters of two to three rods or toroids, were observed (Figure 3(B)). At a 10:1 N:P ratio, individual toroids, which rarely formed clusters, were observed (Figure 3(C)) and structures that resembled elongated or distorted toroids were frequently present, while rod-like structures were rarely observed. Of the PAMAM G1/DNA complexes formed at a 10:1 N:P ratio approximately 40% were individual toroids ranging between 35 and 110 nm and had a mean diameter of 61 ± 14 nm (mean ± SD). We next determined the morphology of dendrimer/DNA complexes formed by 8^+ Arginine. At a 1:1 N:P ratio, an extensive netted or meshwork structure was observed (Figure 3(D)) similar to that seen with PAMAM G1 at this ratio (Figure 3(A)). At a 5:1 N:P ratio elongated and segmented

Table 1. Time-dependency of PAMAM G1/DNA complexation (10:1 N:P ratio)

Incubation time (min)	% Toroids[a]	Mean diameter of toroids[a] (nm; mean ± SD)	% Rods
10	16	64 ± 10	7
20	32	64 ± 11	10
30	35	69 ± 11	3
45	26	62 ± 9	24
60	25	67 ± 8	30
120	21	79 ± 15	41

[a] $n = 100$ at each time point.

structures were observed (Figure 3(E)), whereas at 10:1 toroid-like structures, present almost exclusively in clusters, were observed (Figure 3(F)). Of 8^+ Arginine/DNA complexes formed at a 10:1 N:P ratio, approximately 46% comprised clusters of toroids and 15% comprised individual toroids with a mean diameter 67 ± 17 nm (mean ± SD). For both PAMAM G1/DNA and 8^+ Arginine/DNA complexes, other shapes observed were elongated and distorted toroids or pleiomorphic.

To better understand the behavior and stability of dendrimer/DNA complexes, a time-course study was performed comparing PAMAM G1 and 8^+ Arginine where morphology was observed 10, 20, 30, 45, 60 and 120 min after addition of DNA to dendrimers at a 10:1 N:P ratio. Between 10 and 30 min, PAMAM G1/DNA comprised primarily toroids with few rods (Table 1). The proportion of rods then increased and outnumbered toroids at 60 and 120 min (Table 1). For 8^+ Arginine/DNA at a 10:1 N:P ratio, we observed clusters of toroids and this changed little over time, however, toroids appeared most numerous between 20 and 30 min after DNA/dendrimer mixing (Table 2). Overall, both PAMAM G1/DNA and 8^+ Arginine/DNA formed 'toroidal' structures

Table 2. Time-dependency of 8^+ Arginine/DNA complexation (10 : 1 N : P ratio)

Incubation time (min)	% Toroids[a]	Mean diameter of toroids[a] (nm; mean ± SD)	% Rods
10	27	80 ± 14	0
20	35	68 ± 16	0
30	35	74 ± 13	0
45	27	71 ± 15	0
60	22	76 ± 15	0
120	20	81 ± 13	0

[a] $n = 100$ at each time point.

at all time points tested. However, 8^+ Arginine/DNA showed a disposition to form clusters of toroids, while PAMAM G1/DNA formed individual toroids. On the basis of the time-course study, complexes between DNA and asymmetric dendrimers formed toroids that were stable over the time period tested.

Asymmetric Dendrimers Effectively Complex DNA in Physiological Salt Solutions

For effective gene transfer *in vitro* or *in vivo*, dendrimer/DNA complexes must be stable in physiological salt solutions. Therefore, we next established whether ions present in phosphate buffer (PB) or sodium chloride-containing PBS could interfere with dendrimer/DNA complexation. To this end, the EtBr assay was used to compare complexation of DNA by dendrimers in saline, PB and PBS. When complexed in saline and PB, PAMAM G1 inhibited EtBr fluorescence indicating complex formation, whereas complexes formed in PBS inhibited EtBr fluorescence only when a high N : P ratio of 50 : 1 was used (Figure 4(A)). Similarly, 8^+ Arginine effectively complexed DNA in water, saline and PB as indicated by the EtBr assay (Figure 4(B)). Likewise, for 8^+ Arginine in PBS, EtBr fluorescence was inhibited when a high N : P ratio of 100 : 1 was tested signifying efficient complexation. This data suggest that counterions present within the solvent influence DNA complexation by asymmetric dendrimers and that the presence of the ions in PBS hinders effective complexation at low N : P ratios.

Asymmetric Dendrimer/DNA Complexes Exhibit Minimal Cytotoxicity

To establish the cytotoxicity profile, DNA complexed with PAMAM, asymmetric dendrimers or Lipofectamine® were incubated with HEK 293T cells for 4 h and cell viability was tested using a FACS-based propidium iodide assay a further 20 h later. PAMAM G1/DNA complexes exhibited minimal cytotoxicity to HEK 293T cells at all N : P ratios tested up to 100 : 1 (Figure 5). This was in distinct contrast to Lipofectamine®, which killed approximately 40% of cells under the same conditions. A higher-generation PAMAM dendrimer (G4) was also tested at an N : P ratio of 10 : 1 and this resulted in approximately 20% cell death which increased to approximately 60% when the N : P ratio was increased to 100 : 1(data not shown). In contrast, 8^+ Arginine/DNA at all N : P ratios tested ($\leq$100 : 1 N : P ratio) showed low cytotoxicity with cell viabilities in the range of 90–98% (Figure 5). The data suggest that even at high N : P ratios required for complete complexation of DNA, low-generation asymmetric peptide dendrimers display negligible cytotoxicity when tested in this manner.

Discussion

In vivo use of commercially available high-generation (G4–G10) PAMAM and other spherical dendrimers is limited by cytotoxicity due to their high-cationic charge density, while attempts to functionalize these systems with targeting moieties unavoidably generates heterogeneous end-products. We propose that low-generation asymmetric dendrimers, which are devoid of cytotoxicity and that permit site-specific attachment of a targeting ligand, distal to the site of DNA complexation would be a viable alternative to currently available symmetrical dendrimers. We report the synthesis and characterization of novel asymmetric low-generation dendrimers that effectively complex DNA and exhibit low cytotoxicity particularly when compared to the widely used transfection agent Lipofectamine®, even when complexed with DNA at high N : P ratios.

Fmoc-based SPPS, a relatively simple and cost-effective synthesis method was used to construct the asymmetric dendrimers and post-synthesis analysis by ESI^+-MS and NMR spectra confirmed that the dendrimers synthesized corresponded to the intended structures shown in Figure 1 (1-2–1–5). We conclude that the results of the EtBr assay and TEM imaging indicate that, dependent on the number and nature of terminal amines, low-generation asymmetric dendrimers can effectively complex plasmid DNA with 8^+ Arginine in particular, most efficiently complexing DNA.

The TEM study performed here showed the presence of clusters of toroids formed by 8^+ Arginine/DNA. This is consistent with previous demonstrations that toroids form upon polycation and DNA complexation [33,36–40] and these generally range from approximately 40–90 nm in diameter [37,38,41]. We selected a wider range (35–110 nm) here to ensure all toroids that fell in the 40–90 nm ranges were included for quantitation. In TEM images of 8^+ Arginine/DNA complexes, toroids existed primarily in clusters, whereas PAMAM G1 formed primarily 'non-clustering' toroids. Differences in the propensity to form 'clustering' toroids could be attributable to the marked differences in the physico-chemical properties of asymmetric and spherical dendrimers. For example, asymmetric dendrimers, due to the potentially-fixed stereochemistry of amide bonds formed between the constituent amino acids and the 'polarised' nature of the molecule with terminal amines concentrated in the 'head' region, may permit more interaction between the 'tails' than is possible for spherical dendrimers which exhibit a more uniform arrangement of terminal amines. Although there are reports of PAMAM G1 complexing DNA this has been seen only when PAMAM G1 is used in conjunction with lipid or other cationic helper molecules [42–44]. To our knowledge, this is the first detailed report demonstrating formation of toroidal dendrimer/DNA complexes by PAMAM G1 in the absence of helper molecules. The subtle irregularities in the size and shape of the toroids and rods we observed for dendrimer/DNA complexes are similar to those reported in the literature for other systems [38], and such variations in the morphology of dendrimer/DNA complexes appear normal. On the basis of our time-course studies, we found that there was little difference in the morphology of dendrimer/DNA complexes across the time points tested. However, for PAMAM G1/DNA complexes a difference was noted in the proportion of rods to toroids which increased from 30 min after mixing of PAMAM and DNA. This suggests the optimal incubation time for PAMAM G1/DNA complexes beyond which their morphology reverts to rods is around 30 min. However, with increasing time there was little difference in the morphology of 8^+ Arginine/DNA complexes

Journal of PeptideScience

suggesting an extended period of stability for these complexes, relative to PAMAM G1/DNA complexes.

For TEM, we tested 8^+ Arginine/DNA at various N : P ratios (data not shown) but chose to work with an N : P ratio of 10 : 1 as at higher N : P ratios, the fixed concentration of DNA led to dendrimer/DNA complexes becoming more sparsely distributed on TEM grids. In addition, we also found that increasing dendrimer concentration above 1 mg/ml resulted in large-scale aggregation. Although aggregation of dendrimer/DNA complexes has not been reported in TEM analysis, PAMAM dendrimers ($\geq$G1) have been shown to cause cell damage *in vitro* at concentrations >1 mg/ml [13], and this may reflect findings similar to ours. Therefore, we conclude the optimal dendrimer concentration for forming complexes with DNA is 1 mg/ml for the asymmetric dendrimers tested here.

A hierarchy of complexing effectiveness was observed among the arginine and lysine series of asymmetric dendrimers, with the arginine series complexing DNA with apparently greater affinity than lysine. Others have reported similar or more efficient DNA complexation by arginine termini relative to lysine or other amino acids [45–47]. Arginine possesses a guanidinium moiety, which, with a pKa $\approx$ 13 [48] is protonated over a wide pH range [49]. Guanidinium groups and DNA form characteristic pairs of parallel hydrogen bonds that provide binding strength by their charge and structural organization. These features are consistent with the demonstrated role for guanidinium groups in the arginine amino acid residues playing key roles in DNA binding by proteins, such as histones. Furthermore, because of it's high pKa, arginine can also buffer the endosomal environment, a crucial factor in promoting release of DNA from endosomal compartment, so transfection can take place [50]. Therefore, likely advantages of arginine-containing dendrimers are not only that DNA binding should be relatively insensitive to pH variations during *in vitro* transfer and intracellular trafficking [49] but that they should also increase transfection efficiency.

We established that ions within the solvents used for asymmetric dendrimer/DNA complexation can adversely affect their formation. Although a slight inhibition in dendrimer/DNA complex formation was observed in the presence of PB or NaCl solutions, this was minor. Previous studies have shown that polyamine–DNA complexation can be inhibited by a high concentration of Na^+ ions ($>$1200 mM) [51–53]. The process underlying polyamine-DNA complexation is primarily electrostatic in nature, and is assisted by their net opposite charge. Counterions such as Na^+ present in polyamine–DNA complex solution bind and neutralize the negative (phosphate) charge on DNA thereby reducing its potential to bind polyamines [52]. In the case of PBS as a solvent, and at a low N : P ratio, we can infer that the Na^+ ions neutralize the negative (phosphate) charge on DNA and upon increasing N : P ratio, the effect of Na^+ ions inhibiting dendrimer-DNA complexation is suppressed. However, this would be unlikely to affect the use of asymmetric dendrimers where physiological salt solutions are required as we demonstrated that complexes formed at a high N : P ratio did not result in dissociation of DNA from dendrimer. Therefore, asymmetric dendrimers would be suitable for *in vitro* and *in vivo* use.

Our data demonstrates that both low-generation asymmetric dendrimer/DNA complexes and PAMAM G1/DNA complexes exhibit low cytotoxicity. These findings are consistent with a previous report in which PAMAM G1, but not higher-generation (up to G4) PAMAM dendrimers exhibited little cytotoxicity *in vitro* [13]. A statistically significant reduction in the cell viability (9%; Figure 5) was noted at a 100 : 1 N : P ratio (70 µg/ml dendrimer) of the PAMAM G1 dendrimer, when compared to 5 : 1 N : P ratio (4 µg/ml dendrimer). This is most likely due to the high-cationic charge density present at the high N : P ratio of 100 : 1 that caused cytotoxicity. Overall, the low-generation asymmetric dendrimers described here exhibit low cytotoxicity. Our findings are supported by a recent publication demonstrating that peptide dendrimer (G3 and G5) exhibited low cytotoxicity [4]. An important safety advantage of asymmetric dendrimers described here is that, asymmetric dendrimers will be degraded to harmless natural amino acids, whereas PAMAM dendrimers, upon degradation, may form toxic methacrylates.

In conclusion, the studies described here demonstrate that peptidic asymmetric dendrimers can be constructed with ease, exhibit minimal cytotoxicity and effectively complex DNA. We propose that peptidic asymmetric dendrimer/DNA complexes engineered using SPPS are a new dendrimer family that, when suitably modified and targeted by a range of ligands, will be an effective system for efficient and safe DNA delivery *in vivo*.

Acknowledgements

We thank Dr Tri Le for assisting with NMR assignments. We would also like to thank Dr Matthias Floetenmeyer for providing carbon coated grids and Dr Richard Webb for technical assistance with TEM imaging.

Supporting information

Supporting information may be found in the online version of this article.

References

1. Haensler J, Szoka Jr FC. Polyamidoamine cascade polymers mediate efficient transfection of cells in culture. *Bioconjugate Chem.* 1993; **4**: 372–379.
2. Lungwitz U, Breunig M, Blunk T, Gopferich A. Polyethylenimine-based non-viral gene delivery systems. *Eur. J. Pharm. Biopharm.* 2005; **60**: 247–266.
3. Ohsaki M, Okuda T, Wada A, Hirayama T, Niidome T, Aoyagi H. *In vitro* gene transfection using dendritic poly(L-lysine). *Bioconjugate Chem.* 2002; **13**: 510–517.
4. Luo K, Li C, Wang G, Nie Y, He B, Wu Y, Gu Z. Peptide dendrimers as efficient and biocompatible gene delivery vectors: Synthesis and *in vitro* characterization. *J. Controlled Release* 2010; DOI:10.1016/j.physletb.2003.10.071.
5. Dufes C, Uchegbu IF, Schatzlein AG. Dendrimers in gene delivery. *Adv. Drug Delivery Rev.* 2005; **57**: 2177–2202.
6. Balogh LP, Nigavekar SS, Sung LY, Balogh P, Shi XY, Cook AT, Minc LD, Khan MK. Development of radioactive gold-dendrimer nanocomposite devices to treat tumor microvasculature: Synthesis and biodistribution. *J. Nucl. Med.* 2003; **44**: 1094.
7. Boas U, Heegaard PMH. Dendrimers in drug research. *Chem. Soc. Rev.* 2004; **33**: 43–63.
8. Herborn CU, Barkhausen J, Paetsch I, Hunold P, Mahler M, Shamsi K, Nagel E. Coronary arteries: Contrast-enhanced MR imaging with SH L 643A – Experience in 12 volunteers. *Radiology* 2003; **229**: 217–223.
9. Tomalia DA. Starburst(R) dendrimers – Nanoscopic supermolecules according dendritic rules and principles. *Macromol. Symp.* 1996; **101**: 243–255.
10. Hawker CJ, Frechet JMJ. Preparation of polymers with controlled molecular architecture – A new convergent approach to dendritic macromolecules. *J. Am. Chem. Soc.* 1990; **112**: 7638–7647.
11. Eichman JD, Bielinska AU, Kukowska-Latallo JF, Baker JR Jr. The use of PAMAM dendrimers in the efficient transfer of genetic material into cells. *Pharm. Sci. Technol.* 2000; **3**: 232–245.

12. Roberts JC, Bhalgat MK, Zera RT. Preliminary biological evaluation of polyamidoamine (PAMAM) Starburst(TM) dendrimers. *J. Biomed. Mater. Res.* 1996; **30**: 53–65.
13. Malik N, Wiwattanapatapee R, Klopsch R, Lorenz K, Frey H, Weener JW, Meijer EW, Paulus W, Duncan R. Dendrimers: Relationship between structure and biocompatibility *in vitro*, and preliminary studies on the biodistribution of I-125-labelled polyamidoamine dendrimers *in vivo*. *J. Controlled Release* 2000; **65**: 133–148.
14. KukowskaLatallo JF, Bielinska AU, Johnson J, Spindler R, Tomalia DA, Baker JR. Efficient transfer of genetic material into mammalian cells using Starburst polyamidoamine dendrimers. *Proc. Natl. Acad. Sci. U. S. A.* 1996; **93**: 4897–4902.
15. Braun CS, Vetro JA, Tomalia DA, Koe GS, Koe JG, Middaugh CR. Structure/function relationships of polyamidoamine/DNA dendrimers as gene delivery vehicles. *J. Pharm. Sci.* 2005; **94**: 423–436.
16. Svenson S, Tomalia DA. Dendrimers in biomedical applications – Reflections on the field. *Adv. Drug Delivery Rev.* 2005; **57**: 2106–2129.
17. Krishna TR, Jain S, Tatu US, Jayaraman N. Synthesis and biological evaluation of 3-amino-propan-1-ol based poly(ether imine) dendrimers. *Tetrahedron* 2005; **61**: 4281–4288.
18. Boyd BJ. Past and future evolution in colloidal drug delivery systems. *Expert Opinion on Drug Delivery* 2008; **5**: 69–85.
19. Merritt AT. Solution phase combinatorial chemistry. *Comb. Chem. High Throughput Screening* 1998; **1**: 57–72.
20. Merrifield RB. Solid phase peptide synthesis. I. The synthesis of a tetrapeptide. *J. Am. Chem. Soc.* 1963; **85**: 2149–2154.
21. Chan WC, White PD. Basic principles. *In Fmoc solid phase peptide synthesis : A practical approach*. Oxford University Press: New York, 2000; 9–40.
22. Atherton E, Sheppard RC. Solid phase synthesis-The Merrifield technique and Fluorenylmethoxycarbonyl (Fmoc) amino acids. *In Solid phase peptide synthesis : A practical approach*. IRL Press at Oxford University Press: Oxford, England; New York, 1989; 13–37 and 47–61.
23. Sheppard R. The fluorenymethoxycarbonyl group in solid phase synthesis. *J. Pept. Sci.* 2003; **9**: 545–552.
24. Kumar P, Ban HS, Kim SS, Wu HQ, Pearson T, Greiner DL, Laouar A, Yao JH, Haridas V, Habiro K, Yang YG, Jeong JH, Lee KY, Kim YH, Kim SW, Peipp M, Fey GH, Manjunath N, Shultz LD, Lee SK, Shankar P. T cell-specific siRNA delivery suppresses HIV-1 infection in humanized mice. *Cell* 2008; **134**: 577–586.
25. Roberts JC, Adams YE, Tomalia D, Mercer-Smith JA, Lavallee DK. Using starburst dendrimers as linker molecules to radiolabel antibodies. *Bioconjugate Chem.* 1990; **1**: 305–8.
26. Fajac I, Briand P, Monsigny M. Gene therapy of cystic fibrosis: The glycofection approach. *Glycoconjugate J.* 2001; **18**: 723–729.
27. Parekh HS. The advance of dendrimers – A versatile targeting platform for gene/drug delivery. *Curr. Pharm. Des.* 2007; **13**: 2837–2850.
28. Mutalik S, Hewavitharana AK, Shaw PN, Anissimov YG, Roberts MS, Parekh HS. Development and validation of a reversed-phase high-performance liquid chromatographic method for quantification of peptide dendrimers in human skin permeation experiments. *J. Chromatogr. B* 2009; **877**: 3556–3562.
29. Parekh HS, Marano RJ, Rakoczy EP, Blanchfield J, Toth I. Synthesis of a library of polycationic lipid core dendrimers and their evaluation in the delivery of an oligonucleotide with hVEGF inhibition. *Bioorg. Med. Chem.* 2006; **14**: 4775–4780.
30. URL: http://www.thermo.com/eThermo/CMA/PDFs/Various/File_24 255.pdf [last accessed November 2010].
31. Sarin VK, Kent SBH, Tam JP, Merrifield RB. Quantitative monitoring of solid-phase peptide-synthesis by the ninhydrin reaction. *Anal. Biochem.* 1981; **117**: 147–157.
32. Wiethoff CM, Gill ML, Koe GS, Koe JG, Middaugh CR. A fluorescence study of the structure and accessibility of plasmid DNA condensed with cationic gene delivery vehicles. *J. Pharm. Sci.* 2003; **92**: 1272–1285.
33. Bottcher C, Endisch C, Fuhrhop JH, Catterall C, Eaton M. High-yield preparation of oligomeric C-type DNA toroids and their characterization by cryoelectron microscopy. *J. Am. Chem. Soc.* 1998; **120**: 12–17.
34. Bloomfield VA. Condensation of DNA by multivalent cations – considerations on mechanism. *Biopolymers* 1991; **31**: 1471–1481.
35. Arscott PG, Ma CL, Wenner JR, Bloomfield VA. DNA condensation by cobalt hexaammine(III) in alcohol-water mixtures – dielectric-constant and other solvent effects. *Biopolymers* 1995; **36**: 345–364.
36. Slita AV, Kasyanenko NA, Nazarova OV, Gavrilova II, Eropkina EM, Sirotkin AK, Smirnova TD, Kiselev OI, Panarin EF. DNA-polycation complexes – Effect of polycation structure on physico-chemical and biological properties. *J. Biotechnol.* 2007; **127**: 679–693.
37. Dunlap DD, Maggi A, Soria MR, Monaco L. Nanoscopic structure of DNA condensed for gene delivery. *Nucleic Acids Res.* 1997; **25**: 3095–3101.
38. Golan R, Pietrasanta LI, Hsieh W, Hansma HG. DNA Toroids: Stages in Condensation. *Biochemistry* 1999; **38**: 14 069–14 076.
39. Martin AL, Davies MC, Rackstraw BJ, Roberts CJ, Stolnik S, Tendler SJB, Williams PM. Observation of DNA-polymer condensate formation in real time at a molecular level. *FEBS Lett.* 2000; **480**: 106–112.
40. Bielinska AU, KukowskaLatallo JF, Baker JR. The interaction of plasmid DNA with polyamidoamine dendrimers: mechanism of complex formation and analysis of alterations induced in nuclease sensitivity and transcriptional activity of the complexed DNA. *Biochim. Biophys. Acta, Gene Struct. Expression* 1997; **1353**: 180–190.
41. Tang MX, Li WJ, Szoka FC. Toroid formation in charge neutralized flexible or semi-flexible biopolymers: potential pathway for assembly of DNA carriers. *J. Gene. Med.* 2005; **7**: 334–342.
42. Takahashi T, Kono K, Itoh T, Emi N, Takagishi T. Synthesis of Novel Cationic Lipids Having Polyamidoamine Dendrons and Their Transfection Activity. *Bioconjugate Chem.* 2003; **14**: 764–773.
43. Ogasawara S, Ikeda A, Kikuchi J. Positive Dendritic Effect in DNA/Porphyrin Composite Photocurrent Generators Containing Dendrimers as the Stationary Phase. *Chem. Mater.* 2006; **18**: 5982–5987.
44. Waengler C, Moldenhauer G, Eisenhut M, Haberkorn U, Mier W. Antibody-dendrimer conjugates: The number, not the size of the dendrimers, determines the immunoreactivity. *Bioconjugate Chem.* 2008; **19**: 813–820.
45. Plank C, Tang MX, Wolfe AR, Szoka FC. Branched cationic peptides for gene delivery: Role of type and number of cationic residues in formation and *in vitro* activity of DNA polyplexes. *Hum. Gene Ther.* 1999; **10**: 319–332.
46. Tziveleka LA, Psarra AMG, Tsiourvas D, Paleos CM. Synthesis and characterization of guanidinylated poly(propylene imine) dendrimers as gene transfection agents. *J. Controlled Release* 2007; **117**: 137–146.
47. Okuda T, Sugiyama A, Niidome T, Aoyagi H. Characters of dendritic poly((L)-lysine) analogues with the terminal lysines replaced with arginines and histidines as gene carriers *in vitro*. *Biomaterials* 2004; **25**: 537–544.
48. Albert A, Goldacre R, Phillips J. The strength of heterocyclic bases. *J. Chem. Soc.* 1948; 2240–2249.
49. Aissaoui A, Oudrhiri N, Petit L, Hauchecorne M, Kan E, Sainlos M, Julia S, Navarro J, Vigneron JP, Lehn JM, Lehn P. Progress in gene delivery by cationic lipids: Guanidinium-cholesterol-based systems as an example. *Curr. Drug Targets* 2002; **3**: 1–16.
50. Lee I, Athey BD, Wetzel AW, Meixner W, Baker JR. Structural molecular dynamics studies on polyamidoamine dendrimers for a therapeutic application: Effects of pH and generation. *Macromolecules* 2002; **35**: 4510–4520.
51. Widom J, Baldwin RL. Cation-induced toroidal condensation of DNA studies with $Co_{3+}(NH_3)_6$. *J. Mol. Biol.* 1980; **144**: 431–453.
52. Manning GS. Molecular theory of polyelectrolyte solutions with applications to electrostatic properties of polynucleotides. *Q. Rev. Biophys.* 1978; **11**: 179–246.
53. Wilson RW, Bloomfield VA. Counter-ion-induced condensation of deoxyribonucleic-acid – light-scattering study. *Biochemistry* 1979; **18**: 2192–2196.

